Equilibrium thermodynamics from basin-sampling

Tetyana V. Bogdan and David J. Wales[a)]
University Chemical Laboratories, Lensfield Road, Cambridge CB2 1EW, United Kingdom

Florent Calvo
Laboratoire de Physique Quantique, IRSAMC, Université Paul Sabatier, 118 Route de Narbonne, F-31062 Toulouse Cedex, France

(Received 19 October 2005; accepted 7 November 2005; published online 23 January 2006)

We present a "basin-sampling" approach for calculation of the potential energy density of states for classical statistical models. It combines a Wang-Landau-type uniform sampling of local minima and a novel approach for approximating the relative contributions from local minima in terms of the volumes of basins of attraction. We have employed basin-sampling to study phase changes in atomic clusters modeled by the Lennard-Jones potential and for ionic clusters. The approach proves to be efficient for systems involving broken ergodicity and has allowed us to calculate converged heat capacity curves for systems that could previously only be treated using the harmonic superposition approximation. Benchmarks are also provided by comparison with parallel tempering and Wang-Landau simulations, where these proved feasible. © *2006 American Institute of Physics*. [DOI: 10.1063/1.2148958]

I. INTRODUCTION

Coarse graining the potential energy surface (PES) by considering stationary points, where the gradient vanishes, provides a powerful framework for analyzing structure, dynamics, and thermodynamics in molecular science.[1] The PES can be formally partitioned into the basins of attraction (or catchment basins[2]) of local minima, which are hypervolumes of configuration space from which minimization leads to a particular minimum. If a steepest-descent procedure is used for minimization, then the basins of attraction cannot interpenetrate.[1] More complex basin boundaries will result for faster minimization techniques,[3,4] but this effect does not appear to cause any problem in practical applications. Defining basins of attraction in this way underlies the basin-hopping global optimization procedure.[5–7]

In the superposition approach to thermodynamics, the microcanonical density of states, or the canonical partition function, is written as a sum over contributions from different local minima by restricting the configuration integral to the corresponding basins of attraction.[1,8] This is not a new idea,[9–16] and it has now been used extensively for a variety of atomic and molecular clusters, as well as for biomolecules.[1] It has recently regained popularity for studies of supercooled liquids and glasses,[17–47] where the local minima are usually referred to as "inherent structures" following Stillinger and Weber.[12,13] The simplest implementation of the superposition approach employs explicit densities of states calculated in the classical harmonic approximation, although anharmonic[48] and quantum[49] calculations have also been reported.

The principal advantages of the superposition approach are that it is generally faster than conventional simulations, and that it is naturally ergodic. Hence, provided that the minima are correctly sampled, this method is suitable for the treatment of quasiergodic systems,[50–55] which pose problems even for techniques such as parallel tempering.[56–60]

The number of stationary points grows at least exponentially with system size,[13,61,62] and it is therefore necessary to devise appropriate sampling and reweighting schemes to use the superposition approach for larger systems.[1,16,63,64] The present contribution describes a new "basin-sampling" method, which combines a uniform sampling of local minima in terms of their potential energy with a novel method for approximating the relative contributions from different local minima. The resulting heat capacity curves are nearly as accurate as those calculated using parallel tempering[56–60] or the Wang-Landau (WL) approach.[65–67] Basin-sampling also proves to be particularly advantageous for systems involving broken ergodicity and has enabled us to calculate converged anharmonic heat capacities for systems that could previously only be treated using the harmonic superposition approximation.

A variety of techniques have previously been employed to analyze the thermodynamics of systems involving long time scales and quasiergodicity, where straightforward importance sampling[68] is ineffective. Examples include J-walking,[69] smart walking,[70] parallel tempering,[56–60] successive umbrella sampling,[71] simulated tempering,[72,73] multicanonical schemes,[74–76] entropic sampling,[77–82] and the Wang-Landau approach,[65,66,83] as well as methods based upon adiabatic switching.[84–87] The present contribution began with an attempt to use the ideas of the smart-darting approach.[88] However, we found that the acceptance probability of moves between the small hyperspheres that are placed at each local minimum to achieve detailed balance was simply too small. Our alternative basin-sampling technique is based on a Wang-Landau calculation of the potential energy density of

[a)]Author to whom correspondence should be addressed. Electronic mail: dw34@cam.ac.uk

local minima, combined with a reformulation of the superposition approach. In particular, we combine the calculated probability distribution of local minima with anharmonic vibrational partition functions for representative basins of attraction. The latter calculations also employ a Wang-Landau sampling approach, this time constrained to a particular local minimum. Applications are presented for a variety of atomic clusters, most of which have multifunnel[1] potential energy landscapes, which cause ergodicity problems. Benchmarks are provided by comparison with parallel tempering and Wang-Landau calculations, where these proved feasible.

Our results rely upon one principal approximation that is used to convert the Wang-Landau weights in the main sampling procedure to obtain the potential energy density of minima. Here we require a measure of the average volume of the basin of attraction for minima in each potential energy bin. We have found that a reasonably accurate value for the relative volumes can be obtained as a by-product of the basin-sampling procedure itself, with no additional computational overhead. For each minimization we simply record the distance between the starting configuration and the final geometry. Accumulating statistics for each potential energy bin provides the required estimate of the average relative volume. The resulting heat capacity curves are generally in quantitative agreement with results obtained from parallel tempering.

The paper is organized as follows. In Sec. II we briefly review the superposition approach and the Wang-Landau sampling for the density of states and we introduce the basin-sampling algorithm for calculation of the density of local minima and the vibrational density of states. In Secs. III and IV we apply basin-sampling to analyze phase changes in several selected clusters and compare its performance with that of the parallel tempering and conventional Wang-Landau Monte Carlo methods.

II. THEORY

A. The superposition approach

In the superposition approach[1] the microcanonical total energy density of states and the canonical partition function are decomposed as

$$\Omega(E) = \sum_a \Omega_a(E), \quad Z(T) = \sum_a Z_a(T), \tag{1}$$

where $\Omega_a(E)$ and $Z_a(T)$ are the density of states and partition function for minimum a, the configuration space integration being restricted to the corresponding catchment basin. The complete sums in Eq. (1) must be sampled appropriately for larger systems, just as standard Monte Carlo and molecular dynamics simulations sample the full configurational or phase space. Corrections for sample incompleteness in the superposition approach have been considered before.[16,89] They use the fact that the probability of the system visiting minimum a in equilibrium is proportional to $\Omega_a(E)$ or $Z_a(T)$. Using harmonic densities of states for each local minimum introduces a further approximation and produces $\Omega_a(E) = (E - V_a)^\kappa / \Gamma(\kappa)(h\bar{\nu}_a)^\kappa$, where κ is the number of vibrational degrees of freedom, and $\bar{\nu}_a$ is the geometric mean vibrational frequency for minimum a.[8] Calculation of $\bar{\nu}_a$ requires a normal mode analysis for each stationary point, which may constitute a significant overhead for large systems. Anharmonic corrections have been considered in previous work on transition valley and well anharmonicity in clusters,[48,90] in estimating the basin free energy of water,[91] and separate partition functions have also been investigated directly using confinement methods.[92,93]

B. Wang-Landau sampling for local minima

The Wang-Landau method[65–67,94–97] is designed to achieve a uniform sampling of microstates in a single run, along with a direct calculation of the density of states. It has been used for lattice models,[97–99] adapted for calculation of free energy profiles along reaction coordinates,[100] and also applied to biomolecules,[101] glassy systems,[102,103] and solid-liquid phase equilibria.[104] The algorithm starts with a uniform estimate for $\Omega(E)$ over a histogram of energy bins. For every state visited the current estimate of $\Omega(E)$ is updated by a multiplicative modification factor f, which acts as a convergence parameter. f is relatively large at the start of a calculation, to allow for rapid accumulation of the histograms over the full energy range, but it is progressively reduced towards unity as the discrete representation of $\Omega(E)$ improves in accuracy. The length of one WL iteration, over which f is fixed, is determined by a predefined convergence criterion, such as the "flatness parameter" $x\%$, the percentage by which histogram entries are allowed to deviate from the mean,[65] or the current value of the modification factor.[105] A discussion of different convergence procedures is presented in Sec. II E. As f approaches a predefined value f_{final}, and provided the random walk is unbiased and all the configurations are sampled uniformly, the density of states $\Omega(E)$ converges to its true value.[65]

C. The basin-sampling algorithm

A successful sampling algorithm for local minima must include a method for making efficient moves in configuration space.[88] To achieve this objective we can simply modify the basin-hopping global optimization procedure[5–7] in a way that preserves detailed balance. In basin hopping, implemented in the public domain GMIN program, the moves between local minima are performed by perturbing all Cartesian coordinates according to displacements drawn from a uniform distribution.[6] We then optimize the geometry to find a local minimum after each such perturbation and accept or reject the step based on a Metropolis scheme, using the energy difference between the new minimum and the old one.[6] This approach essentially performs a Monte Carlo sampling of the transformed PES $\tilde{E}(\mathbf{X}) = \min\{E(\mathbf{X})\}$, where $\mathbf{X}$ represents the vector of nuclear coordinates, and min signifies that an energy minimization is performed starting from configuration $\mathbf{X}$. After accepting a step, it has generally been found that the global optimization procedure is most efficient if the coordinates are set to those of the new minimum.[6,106] However, if we wish to maintain detailed balance then we can simply omit this step and allow the coordinates to vary continuously.

The success of basin-hopping as a global optimization technique is partly due to the transformation of the landscape, which effectively removes transition state regions. Minima can interconvert all along their basin boundaries, and atoms can even pass through each other, because the transformed energy is not the instantaneous value, but the energy obtained after minimization. However, these observations are not sufficient to explain the success of basin-hopping for multifunnel landscapes.[1] In fact, the modified thermodynamics of the transformed landscape results in broadened transitions, so that the occupation probabilities of different morphologies remain significant at temperatures where there is still a good chance that transitions can occur between them.[50]

The present basin-sampling (BS) approach to thermodynamics exploits the above favorable characteristics of basin-hopping global optimization to obtain an ergodic sampling of the potential energy density of local minima $p(V)$, where $p(V)dV$ is the number of minima in the potential energy range from V to $V+dV$. The function $p(V)$ must be clearly distinguished from the total energy density of states $\Omega(E)$ and the configurational density of states $\Omega_c(V)$. Starting from a random configuration we employ a WL approach to calculate $p(V)$, where moves are proposed by random perturbations of all the Cartesian coordinates at once, followed by minimization to find the potential energy of the corresponding local minimum. Hence the procedure is similar to the conventional WL approach, except that the energy bins and histogram are constructed from the potential energies of the local minima found by geometry optimization from the instantaneous configuration. Although it may appear that the minimization conducted at every step is a significant computational burden, just as for basin-hopping global optimization, it turns out to be beneficial.

The potential energy spectrum is bound from below by the energy of the global minimum V_0 and represented by n equally spaced windows, which constitute histogram bins of width ΔV. For a random configuration the average probability of quenching to a minimum with potential energy V in the range $V_j \leqslant V < V_{j+1}$ is $g_j = p_j A_j$, where $V_j = V_0 + j\Delta V$,

$$p_j = \int_{V_j}^{V_{j+1}} p(V')dV', \tag{2}$$

and A_j is the average volume of the basins of attraction in configuration space for minima in this bin.

During the random walk we accumulate statistics for g_j, H_j, and $\bar{H}_j$, where H_j and $\bar{H}_j$ are the number of times the trajectory visits bin j throughout the whole run and during the current WL iteration (with fixed modification factor f), respectively. We start the simulation from a uniform distribution of g_j and multiply g_j by f every time bin j is visited. At each step all Cartesian coordinates are displaced by a random number in the range $[-1,1]$ times the maximum step size, which can be fixed or adjusted to satisfy a predefined value of the acceptance ratio.[6] The perturbations are chosen to preserve the center of mass of the structure to remove the translational degrees of freedom. In our calculations the maximum step size was fixed, but values ranging from 10% to 40% of the equilibrium bond length generally did not have any significant impact on the results. Since the BS steps are between local minima it is possible to use step sizes of two orders of magnitude larger than for parallel tempering and other methods that sample instantaneous configurations. We did not use dynamical step size adjustment because, in contrast to the case of global optimization calculations, such an approach can produce systematic errors and violate detailed balance.[107]

The structure obtained after each geometrical perturbation is minimized using a modified limited-memory Broyden-Fletcher–Goldfarb-Shanno (L-BFGS) algorithm.[108,109] For calculations on finite systems the configuration space is restricted to bound clusters using a spherical container, as in previous work.[16,54,110,111] In the case of an atom leaving the container at any point during the minimization the coordinates are reset to the starting unminimized geometry, and no statistics are updated. If the minimization was successful, the weights of bins j and j', corresponding to the energies of the old and new minima, are compared. If $g_j > g_{j'}$, then we set $\ln g_{j'} \rightarrow \ln g_{j'} + \ln f$, $H_{j'} \rightarrow H_{j'} + 1$, and $\bar{H}_{j'} \rightarrow \bar{H}_{j'} + 1$. If $g_j < g_{j'}$ the corresponding quantities for bin j are modified instead. If the walk goes outside the defined energy range we recount the structure in bin j to avoid boundary effects.[97] In contrast to most basin-hopping global optimization calculations, the coordinates are allowed to vary continuously, as mentioned above.

Our test case studies suggest that it is helpful to choose a starting modification factor proportional to the total number of minima as well as to the number of bins into which the potential energy spectrum is separated. Both theory and empirical evidence suggest that the number of distinct geometrical isomers grows exponentially with the number of atoms, i.e., $N_{\min} = Ae^{\alpha N}$.[61,112] The constants A and α depend upon the potential and can be fitted using known values of $N_{\min}$ for small N. For Lennard-Jones clusters, where nearly complete databases are available for $N \leqslant 16$,[62] the fitted constants are $A = 0.003\,97$ and $\alpha = 0.9897$. Since the sampling does not distinguish between different permutation-inversion isomers, $N_{\min}$ should be further multiplied by $2N!$. (For this estimate we assume that the majority of local minima have point group C_1.) For the BS runs using 100 bins, f_0 ranged from 1.36 for LJ_{13} to 24.84 for LJ_{75} in the present work.

The superposition approximation can be used to represent the density of states and the total canonical partition function as

$$\Omega_c(V) \propto \sum_j p_j \Omega_j^{\text{vib}}(V)\Theta(V - V_j) \tag{3}$$

and

$$Z(T) \propto \sum_j p_j e^{-V_j/k_B T} Z_j^{\text{vib}}(T),$$

where $Z_j^{\text{vib}}(T)$ is the average vibrational partition function for minima in bin j relative to an energy origin at V_j. The analytical factor that arises from the integral over momentum space has been included in $Z_j^{\text{vib}}(T)$. The appropriate weighting for permutation-inversion isomers[1] is included directly in p_j.

The internal energy and heat capacity are obtained from the standard thermodynamical formulas:

$$U(T) = -\frac{\partial \ln Z}{\partial \beta} = \langle E \rangle, \quad C(T) = \frac{\partial U}{\partial T} = \frac{k_B}{T^2}\left(\langle E^2 \rangle - \langle E \rangle^2\right). \tag{4}$$

These expressions involve the canonical averages of the potential energy and its square. In terms of the partition function, the heat capacity reads

$$C(T) = k_B \beta^2 \left[\frac{1}{Z}\frac{\partial^2 Z}{\partial \beta^2} - \frac{1}{Z^2}\left(\frac{\partial Z}{\partial \beta}\right)^2 \right]. \tag{5}$$

Thus the first and second derivatives of Z with respect to β are required. From the general expression of Eq. (3) we find

$$\frac{\partial Z}{\partial \beta} \propto \sum_j \left[-V_j Z_j^{\mathrm{vib}} + \frac{\partial Z_j^{\mathrm{vib}}}{\partial \beta} \right] p_j e^{-V_j/k_B T}, \tag{6}$$

and

$$\frac{\partial^2 Z}{\partial \beta^2} \propto \sum_j \left[V_j^2 Z_j^{\mathrm{vib}} - 2V_j \frac{\partial Z_j^{\mathrm{vib}}}{\partial \beta} + \frac{\partial^2 Z_j^{\mathrm{vib}}}{\partial \beta^2} \right] p_j e^{-V_j/k_B T}. \tag{7}$$

In the harmonic approximation $Z_j^{\mathrm{vib}}(T) = (k_B T/h\bar{\nu}_j)^\kappa$, where $\kappa = 3N-6$ for nonrotating, nontranslating clusters and $\kappa = 3N-3$ for bulk models. The heat capacity resulting from this approximation is given exactly by[16]

$$C(T) = \kappa k_B - \frac{Z^{(1)}(T)^2}{Z^{(0)}(T)^2 k_B T^2} + \frac{Z^{(2)}(T)}{Z^{(0)}(T) k_B T^2}, \tag{8}$$

where $Z^{(s)}(T) = \Sigma_j p_j e^{-V_j/k_B T} (V_j)^s / (h\bar{\nu}_j/k_B T)^\kappa$. The first term in Eq. (8) is the momentum contribution.

To make use of the anharmonic expressions of Eq. (3), which result in Eqs. (6) and (7), it appears that we require both the probabilities p_j and the explicit temperature dependence of the vibrational contributions Z_j^{vib}. However, we have found approximations for both quantities that involve practically no computational overhead, and provide significantly more accurate results than the harmonic approximation.

For each minimization that is performed during the BS run we also calculate the distance between the starting geometry and the structure of the resulting minimum. An average for the accumulated distribution of such distances is calculated for minima in each bin j during the whole run, resulting in a set of values, d_j. We then use d_j^κ as an estimate of the relative catchment basin hypervolumes A_j, giving $p_j \propto g_j/d_j^{\kappa+3}$. This is the first main approximation in the present BS study. Although more accurate methods exist for estimating volumes of convex polytopes, such as the convex hull approach and Voronoi constructions,[113] for general dimensions there are no known polynomial algorithms. The worst-case running time for a convex hull algorithm is of order $\mathcal{O}(d!n^d)$, where d is the number of dimensions, and n is the number of points in the set that is enclosed by the convex hull.[114] For most applications of the BS algorithm the dimensionality of the problem would make any such algorithm computationally unfeasible. Hence, we will simply use the ratio of mean distances in this initial investigation. The distance d_j includes both rotational and vibrational degrees of freedom. To estimate the vibrational contribution alone we accumulate an average δ_j based upon the distance between the instantaneous configuration and the local minimum but minimized with respect to rigid body coordinates.[115] Hence $\delta_j < d_j$, and we generally observed differences of less than 10% between the two quantities for the present systems. The two different distances serve different purposes in our calculations. The heat capacity curves that we will compare with conventional simulations are for nonrotating, nontranslating clusters, where δ_j is used to calculate vibrational partition functions. However, to convert the WL weights in the BS phase of the simulation into the potential energy density of local minima we must use the relative values of $d_j^{\kappa+3}$ for a free cluster. The average value of the distance without removing the overall rotation is required because the steps in configuration space sample over orientations (but not overall translations of the center of mass).

D. Vibrational partition functions

Anharmonic contributions to the partition functions of individual local minima can have a significant effect on thermodynamic properties.[48,116–118] During the BS run we record the number of times a given minimum was found during sampling and save the most frequently encountered minima associated with each potential energy bin. We then perform a more conventional WL sampling of the configuration space associated with each of the minima to calculate an average $\Omega_j^{\mathrm{vib}}(E)$ or the partition function $Z_j^{\mathrm{vib}}(T)$. In order to restrict this calculation to the selected minimum, we impose an additional constraint that the minimized Euclidean distance between each configuration and the local minimum is less than the value of δ_j calculated for the appropriate potential energy bin. This idea is similar to the confinement approach,[119] but without the computationally expensive quenching used to identify the instantaneous catchment basin. With δ_j acting as a "tether" constraining the distance from each local minimum, we aim to sample only the vibrational states associated with a given potential well and hence estimate an average vibrational partition function for each of the original BS bins. Since $\Omega_j^{\mathrm{vib}}(E)$ and $Z_j^{\mathrm{vib}}(T)$ do not include overall rotation we use δ_j rather than d_j to specify the constraint, since δ_j is minimized with respect to the orientational degrees of freedom. Using the results of these tethered WL runs to approximate $\Omega_j^{\mathrm{vib}}(E)$, we can rewrite Eq. (3) as

$$\Omega(E) \propto \sum_{j=1}^{b} \frac{g_j}{d_j^{\kappa+3} m_j} \left\{ \sum_{\ell=1}^{m_j} \sum_{i=1}^{b_j^t} \xi_i(\ell) \Theta\left[E - E_j(\ell)\right] \right\}, \tag{9}$$

where b is the number of potential energy bins in the BS run, m_j is the number of saved minima in BS bin j, b_j^t is the number of bins used in tethered WL runs for minima in BS bin j, and $\xi_i(\ell)$ is the WL weight of bin i in the tethered WL run for minimum ℓ. The canonical partition function follows from Laplace transformation:

$$Z(T) \propto \sum_{j=1}^{b} \frac{g_j}{d_j^{\kappa+3} m_j} e^{-V_j/k_B T} \left\{ \sum_{\ell=1}^{m_j} \sum_{i=1}^{b_j^t} \xi_i(\ell) e^{-V_i(\ell)/k_B T} \right\}. \tag{10}$$

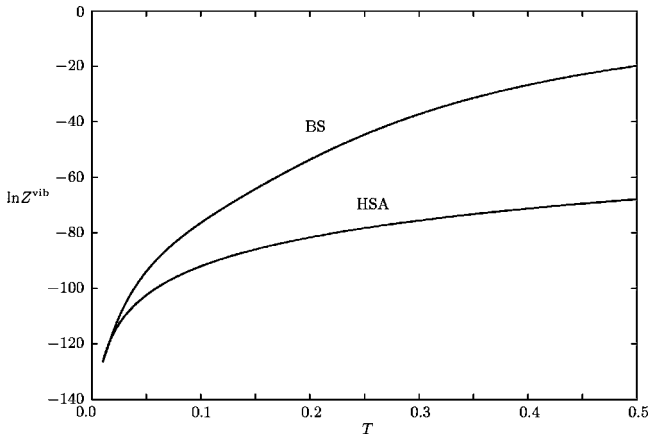

FIG. 1. Temperature dependence of the vibrational partition function Z_{vib} for the basin of attraction associated with the global minimum of LJ_7 calculated using the tethered WL approach (BS) and the harmonic approximation (HSA).

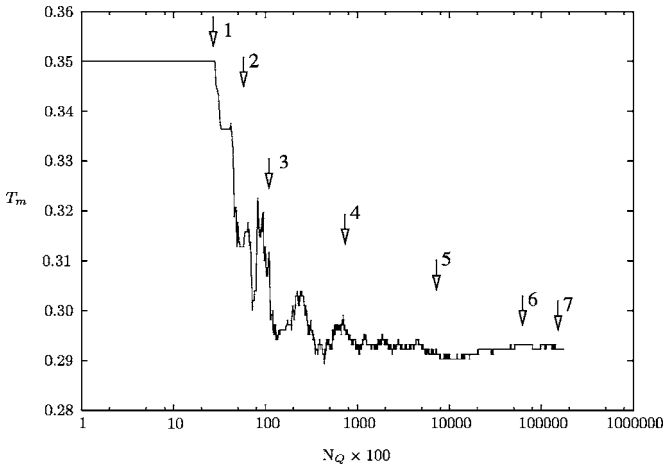

FIG. 2. Convergence of the calculated melting temperature for LJ_{13}, T_m, (R_c=2.3) as a function of the number of quenches N_Q. Arrows and numbers indicate the end of each WL iteration. T_m was calculated after every 100 quenches in the BS phase using vibrational partition functions obtained from a fixed set of local minima in each BS bin.

The starting modification factor for each tethered WL run was estimated from the harmonic vibrational density of states as $f_0 \propto \Omega_h^{\mathrm{vib}}(E^*)^{1/b_j^t}$. Here the value of E^* was set to the upper limit of the potential energy sampled relative to the local minimum in question. This cutoff was chosen as $E^* = V_0 + 3Nk_B T_{\max}$, where V_0 is the potential energy of the global minimum. E^* also coincides roughly with the average potential energy of the highest temperature trajectory in parallel tempering (PT) calculations of the same system (for example, $T_{\max} \simeq 0.5$ for LJ clusters). The step size in configuration space used in the tethered WL runs was typically a factor of 100 smaller than for the BS phase of the calculation and was comparable to the value employed in conventional PT or WL simulations.

To speed up the tethered WL calculations we used the harmonic vibrational density of states to initialize the histogram for the first minimum considered in each BS bin. For subsequent minima in the same BS bin we used the converged density of states from the previous minimum as the starting density. This phase of the calculation can be run independently of the basin-sampling part, and tethered WL runs for different minima can be distributed over different processors on a parallel computer. We found that it was generally sufficient to save three of the most frequently encountered local minima per BS bin, and the tethered WL part of the calculation required less computer time than the initial BS phase. The convergence problems of the WL method for continuous systems[95] were resolved using an overlapping window approach, since the vibrational density of states is a smooth function of the potential energy. We have found that it is advisable to update the density of states of the current state if the potential energy of the suggested state lies outside the energy window, and failure to do so can lead to a significant underestimation of $\Omega_j^{\mathrm{vib}}(E)$ at the boundaries of the window. Figure 1 shows the resulting vibrational partition function $Z^{\mathrm{vib}}(T)$ for the global minimum of LJ_7 calculated using the tethered WL method. For comparison we also present $Z^{\mathrm{vib}}(T)$ calculated within the harmonic approximation. As expected, the results agree in the low temperature limit, but there are significant discrepancies at higher temperatures. Finally, the derivatives of Z_j^{vib} with respect to β, needed to calculate the heat capacity, are obtained straightforwardly as

$$Z_j^{\mathrm{vib}} = \frac{1}{m_j} \sum_{\ell=1}^{m_j} \sum_{i=1}^{b_j^t} \xi_i(\ell) e^{-\beta V_i(\ell)},$$

$$\frac{\partial Z_j^{\mathrm{vib}}}{\partial \beta} = \frac{1}{m_j} \sum_{\ell=1}^{m_j} \sum_{i=1}^{b_j^t} -V_i(\ell) \xi_i(\ell) e^{-\beta V_i(\ell)}, \tag{11}$$

$$\frac{\partial^2 Z_j^{\mathrm{vib}}}{\partial \beta^2} = \frac{1}{m_j} \sum_{\ell=1}^{m_j} \sum_{i=1}^{b_j^t} [V_i(\ell)]^2 \xi_i(\ell) e^{-\beta V_i(\ell)}.$$

E. Optimizing the convergence

We have used a variety of techniques to verify the convergence of both the WL scheme employed in the initial BS phase and the tethered WL runs used to calculate individual vibrational partition functions for local minima. In particular, we have compared a histogram flatness condition,[65,66] histogram saturation,[120] and the proportionality between the minimal number of hits and the current modification factor.[105] Zhou and Bhatt have proved that the density of states is sufficiently converged for a given value of the modification factor if the average number of visits to each bin[105] $\langle \bar{H}_j \rangle > 1/\sqrt{\ln f}$. In this procedure every WL iteration is exponentially more expensive than the previous one, which makes it more time consuming per iteration than other convergence criteria (Fig. 2). However, we have found that it provides the smoothest convergence of the density of states and thermodynamic properties for our test cases. Hence fewer WL iterations are required, and the overall computer time is minimized (Fig. 3).

Because the energy spectrum for local minima is discrete in the initial BS phase, some BS bins may never be visited. The WL convergence criterion was modified to ignore such bins. At the end of each WL iteration, the modification factor

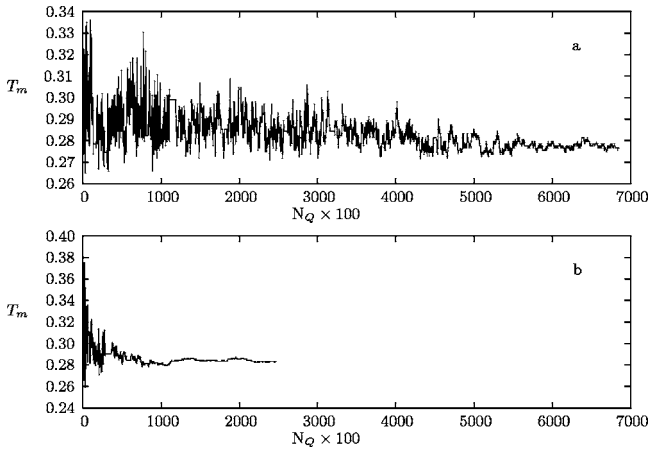

FIG. 3. Convergence of the melting temperature T_m for LJ_{13} ($R_c=1.8$) as a function of the number of quenches N_Q using two different histogram convergence procedures: (a) using a histogram flatness condition of 20% for 100 bins and (b) ensuring that the minimal number of visits to each bin is proportional to $1/\sqrt{\ln f}$ condition for the same number of bins. For both simulations, 10 WL iterations were performed.

was reduced to $f^{1/10}$ in both BS and tethered WL runs, and we usually needed between 6 and 10 WL iterations for the heat capacity curve to converge. We have also tested the histogram saturation stopping condition[120] and have found that for LJ clusters convergence of histogram saturation values, defined as $\Delta\bar{H}=\Sigma_j\bar{H}_j-\min\bar{H}_j$, also correlates with convergence of the density of states. In agreement with the results for the lattice models in Ref. 120, the dependence of the modification factor on the number of visits in one WL run was found to be roughly linear (Fig. 4).

III. TEST SYSTEMS

Atomic clusters provide an ideal testing ground for the BS method, especially with the advent of new experiments to probe such systems.[121,122] In particular, clusters bound by the Lennard-Jones (LJ) potential exhibit a wide range of interesting behavior. The heat capacities for LJ_N clusters with

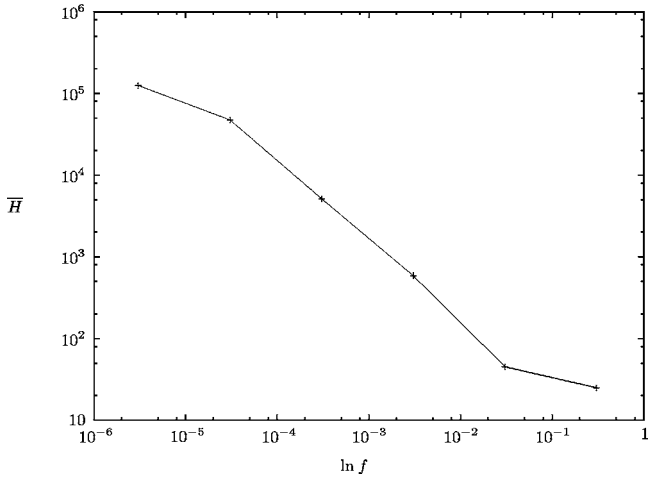

FIG. 4. Number of quenches during one WL iteration $\bar{H}$ as a function of the modification factor $\ln f$.

$4<N<60$ have previously been calculated using J-walking and PT;[111,123] phase changes in larger ($N<147$) clusters have also been studied using PT.[124]

The topology of the PES for clusters such as LJ_{38} and LJ_{75} presents particularly difficult sampling problems.[1] For LJ_{38} the global minimum, a truncated octahedron, is located at the bottom of a narrow potential energy "funnel"[1] and is separated from the next-lowest potential energy minimum (based upon icosahedral packing) by large potential and free energy barriers.[52] Systems with such double-funnel landscapes are especially prone to trapping and quasiergodic behavior.[1,125] If one morphology is favored by entropy and the other by a lower potential energy, then a low temperature solid-solid-like transition may occur when the global free energy minimum changes.[1,53] This behavior has been analyzed using harmonic superposition,[126] multicanonical,[52] and PT calculations,[54,55] which all reveal a feature in the heat-capacity curve that corresponds to the finite system analog of a solid-solid phase transition.

For LJ clusters the PES is defined by the potential[127]

$$V=4\varepsilon\sum_{i<j}\left[\left(\frac{\sigma}{r_{ij}}\right)^{12}-\left(\frac{\sigma}{r_{ij}}\right)^{6}\right], \tag{12}$$

where ε and $2^{1/6}\sigma$ are the pair equilibrium well depth and separation, respectively. We will employ reduced units, i.e., $\varepsilon=\sigma=1$, throughout and define the reduced temperature as k_BT/ε.

Alkali halide clusters were modeled by the Coulomb plus Born-Mayer potential using the Tosi-Fumi parametrization[128]

$$V=\sum_{i<j}\left[\frac{q_iq_j}{r_{ij}}+A_{ij}\exp^{-r_{ij}/\rho}\right], \tag{13}$$

where q_i is the charge of atom i, r_{ij} is the distance between the ions, and A_{ij} and ρ are the ionic interaction parameters ($A_{++}=15.564$, $A_{--}=128.049$, $A_{+-}=46.106$, and $\rho=0.599\,04$ are relevant values for NaCl). Atomic units were used throughout for this potential.

IV. RESULTS

To provide suitable benchmarks for the BS results we have calculated heat capacity curves for LJ_{13}, LJ_{31}, LJ_{38}, and LJ_{55} and compared them with PT (Refs. 54 and 55) and superposition calculations.[1] We have also explored the thermodynamic properties of LJ_{75} and the ionic clusters $(NaCl)_4$, $(NaCl)_{13}Na^+$, and $(NaCl)_{32}$.

The PT simulations were performed using 50 replicas for LJ clusters and 30 replicas for NaCl clusters. The number of MC steps required per replica depended strongly on the cluster. For systems with a single-funnel energy landscape convergence is easily achieved. In contrast, clusters such as LJ_{38} require a significant numerical effort in order to obtain stable results for the melting point and more specifically for the structural transition temperatures. The replica temperatures were allocated regularly, with a couple of extra trajectories at low temperatures to make exchange moves easier. We did not attempt to use other temperature schedules (such as a

TABLE I. Melting temperatures T_m for selected test systems obtained with basin-sampling (BS), compared to a variety of alternative approaches: HSA indicates the harmonic superposition approximation using a sample of local minima obtained by quenching from molecular dynamics trajectories, ASA indicates a second-order anharmonic superposition approximation using a sample of local minima (Ref. 90), PT indicates parallel tempering (Refs. 56–60), and WL is the original Wang-Landau implementation (Ref. 65). For systems that exhibit a low temperature solid-solid transition the two peak positions are reported. The last two columns show the deviations of the melting temperature ΔT_m and the height of the heat capacity ΔC_v predicted by BS from the PT results. Where applicable, in the pair of numbers separated by commas the first corresponds to the solid-solid transition values.

System	HSA	ASA	PT	WL	BS	ΔT_m (%)	ΔC_v (%)
LJ_{13}	0.3512	0.2869	0.2887	0.2949	0.2891	0.01	18
LJ_{31}	⋯	⋯	0.03; 0.32	0.03; 0.35	0.03; 0.30	0.1, 3	2, 16
LJ_{38}	0.12; 0.18	0.11; 0.17	0.11; 0.164	0.09; 0.159	0.11; 0.156	0.1, 5	1.6, 8
LJ_{55}	0.3427	0.2985	0.2946	0.241	0.2963	0.3	7
LJ_{75}	0.08; ⋯	⋯	⋯	⋯	0.13; 0.310	⋯	⋯
$(NaCl)_{32}$	⋯	⋯	752 K	⋯	792 K	5	2

geometric distribution), because we wanted to cover the entire temperature range without any prior knowledge of the melting point.

The conventional Wang-Landau simulations were performed by discretizing the potential energy range into 500 identical bins, starting with a modification factor $f_0=e$. At each iteration convergence was monitored by examining the average number of visits to each bin, and the next iteration was started once this number exceeded $1/\sqrt{\ln f}$. Except for LJ_{13}, this condition was never fully satisfied, and instead we stopped the calculation once a maximum number of 10^9 steps had been performed. Even for the very simple $(NaCl)_4$ case, which only has two different isomers, we were not able to sample the configuration space efficiently using the conventional Wang-Landau method, hence the CPU times reported in Table II are lower bounds to the actual times required for convergence. Current implementation of PT appears to be significantly more efficient that conventional WL for these tests. Clearly, methodological improvements along the lines of Ref. 120 are needed for the WL method to become useful for atomic clusters.

A. LJ_{13}

The global minimum for LJ_{13} is a complete Mackay icosahedron.[129] The corresponding potential energy landscape can be described as a single "palm tree,"[1] indicating that efficient relaxation to the global minimum will occur over a wide range of total energy or temperature. An essentially complete set of local minima is available for this system, and accurate thermodynamic properties have previously been calculated using a variety of techniques.[110,123]

Results for LJ_{13} are presented in Table I and Fig. 5. The predicted melting temperature T_m defined as the temperature above which the liquidlike phase becomes accessible agrees quantitatively with both PT and previous anharmonic superposition results.[48] The same confining sphere radius of $R_c=1.8$ was used in the BS and PT calculations, since this parameter is known to affect the results.[110,123] Table II presents comparisons between the performances of BS, PT, and the original WL implementation.

The small size of LJ_{13} allowed us to carry out extensive tests of the BS method, which enabled us to infer optimal parameters for calculations on more difficult systems. For example, Fig. 6 illustrates how the number of quenches necessary to achieve convergence scales with various BS input parameters.

Figure 6 indicates that the choice of the BS bin width, which in turn determines the number of bins used, can significantly affect the convergence. The computational cost grows as the bin width decreases, because it becomes harder

TABLE II. Convergence times (in seconds and hours) for BS, PT, and the original WL sampling technique. For PT the simulations were based on M equally spaced temperature trajectories, with P MC cycles, which followed Q equilibration cycles, hence the notation $M\times(P+Q)$. For WL 15 iterations were used. The convergence criterion was based on ensuring no fewer than $1/\sqrt{\ln f}$ visits were made to each bin. The starting value of f was chosen so that the ratio $1/\sqrt{\ln f}=1$, the ratio was then doubled every WL iteration, reaching 2^{14} for the final WL iteration. 500 equally spaced energy bins were used for all clusters. Convergence was only achieved for LJ_{13}, and the number of MC cycles was otherwise restricted to the maximal number of cycles $P_{\max}$, hence the notation $15\times P_{\max}$. For basin-sampling the column labeled "parameters" contains approximate number of minima included in the sample.

System	Method	Parameters	CPU time
LJ_{13}	PT	$50\ (10^5+2\times10^4)$	1350 s
LJ_{31}	PT	$50\ (10^7+2\times10^6)$	180 h
LJ_{38}	PT	$50\ (10^9+2\times10^8)$	1860 h
LJ_{55}	PT	$50\ (10^6+2\times10^5)$	50 h
$(NaCl)_4$	PT	$30\ (10^5+2\times10^4)$	640 s
$(NaCl)_{13}Na^+$	PT	$30\ (10^6+2\times10^5)$	19 h
$(NaCl)_{32}$	PT	$30\ (10^6+2\times10^5)$	106 h
LJ_{13}	WL	15×10^6	330 s
LJ_{31}	WL	15×10^8	>4 000 h
LJ_{38}	WL	15×10^9	>5 500 h
LJ_{55}	WL	15×10^8	>11 000 h
LJ_{13}	BS	1 200	1500 s
LJ_{31}	BS	45 000	42 h
LJ_{38}	BS	65 000	160 h
LJ_{55}	BS	150 000	65 h
LJ_{75}	BS	1 200 000	433 h

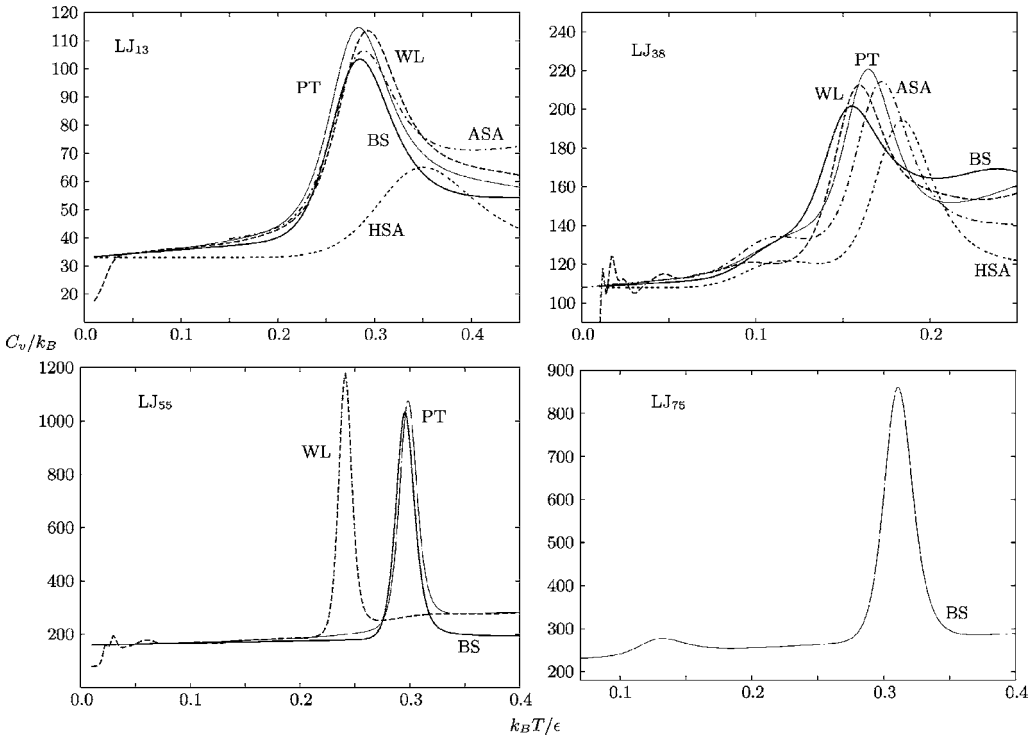

FIG. 5. Heat capacity curves as functions of temperature (in reduced units) for selected LJ clusters. The lines are labeled as follows: HSA indicates the harmonic superposition approximation using a sample of local minima obtained by quenching from molecular dynamics trajectories, ASA indicates a second-order anharmonic superposition approximation using a sample of local minima (Ref. 90), PT indicates parallel tempering, BS is the basin-sampling, and WL is the Wang-Landau sampling.

to satisfy the flatness criterion, which in this case was set to 90%. A reasonable choice of ΔV seems to range from 5% to 12% of the energy spectrum being sampled.

The number of WL iterations is determined by f_{final}, which serves as the convergence criterion. As every subsequent WL iteration becomes more time consuming, it is important to chose f_{final} carefully. In the original WL paper it is recommended that between 18 and 20 WL iterations should be used.[65] We have observed for the majority of systems presented here that 15 iterations or fewer are sufficient to obtain the desired accuracy.

The cost increases significantly with the radius of the constraining sphere, because more and more extended structures are included in the sampling, resulting in a higher T_m. We also observed that the average volume of the basins of attraction grows as R_c increases. For $R_c=1.8$, d for the bin

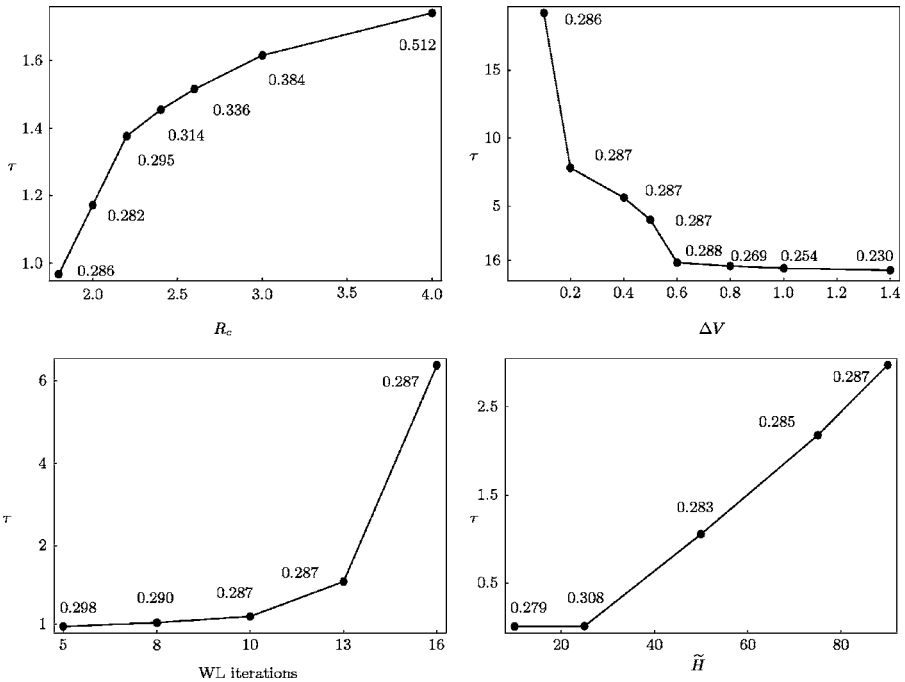

FIG. 6. Dependence of the convergence time τ (measured in millions of energy evaluations) on the BS run parameters for LJ_{13}. R_c is the radius of the confining container, ΔV is the energy bin width, 16 WL iterations correspond to $f_{\text{final}}=1.000\,000\,1$ for the target modification factor, and $\tilde{H}$ (in %) is the histogram flatness parameter. The value of T_m predicted in the corresponding BS run is specified next to each data point.

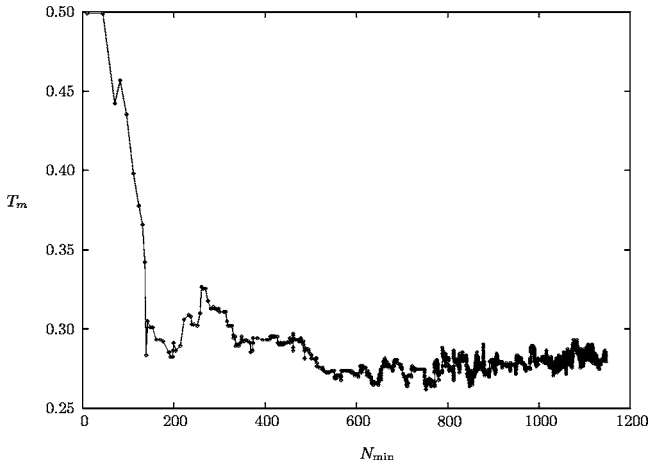

FIG. 7. The predicted melting temperature T_m for LJ_{13} as a function of the number of geometrically distinct isomers sampled, $N_{\min}$.

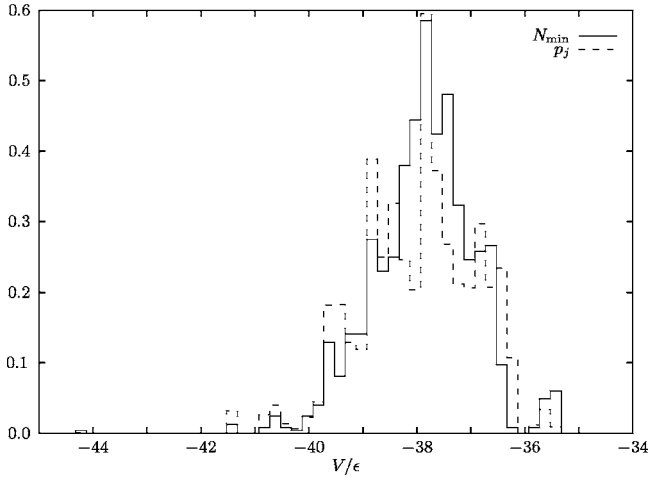

FIG. 8. The calculated potential energy density of minima p_j for LJ_{13} from BS simulations and the density of minima calculated from the practically complete database of LJ_{13} stationary points, $N_{\min}$. In the $N_{\min}$ distribution the contribution of every minimum is scaled by the order of the point group of that minimum to correct for the number of permutation-inversion isomers (Ref. 1). Both distributions are presented as normalized histograms.

containing the global minimum is 2.28, but for $R_c=2.2$, 2.6, and 3.0 it increases to 3.18, 4.21, and 5.30, respectively.

Since a complete sample of local minima is available for LJ_{13}, it was instructive to compare the distributions of the number of minima partitioned into bins and the p_j obtained from BS for the same bin settings. During a BS run, approximately 1200 out of 1517 distinct geometrical minima were found before the convergence criteria were met, but if the simulation was allowed to run longer, almost a complete set of minima was obtained. As expected, though, the density of states in the basin of attraction of the global minimum has the greatest influence on the features of the heat capacity curve in the case of LJ_{13}, and sampling roughly 700 minima was sufficient (see Fig. 7). From Fig. 8, we see that the agreement between the density of states p_j predicted by BS and the histogram of the number of minima in the complete sample is rather good, especially considering the relatively small computational effort involved.

The accuracy of the p_j clearly depends upon the calculation of the volumes of the basins of attraction A_j based upon the average distances d_j. To test this approximation further we have attempted to calculate A_j directly for the four geometrically distinct isomers of LJ_7 by quenching from randomly generated coordinates. We found that the brute force and BS results agree that the highest-energy isomer has a comparatively large weight because of its low point group symmetry, which accounts for the unusual stability of this isomer at higher temperatures.[130]

Figure 9 shows the variation of d_j^{κ} with V_j for four of the LJ clusters. These logarithmic plots indicate an approximate power-law behavior. This property may be connected to the scale-free character observed in the previous network analysis of the PES.[131] The latter work showed that the global minimum generally acts as a highly connected hub, and the degree of connectivity decays as a power law as the potential energy increases.[131]

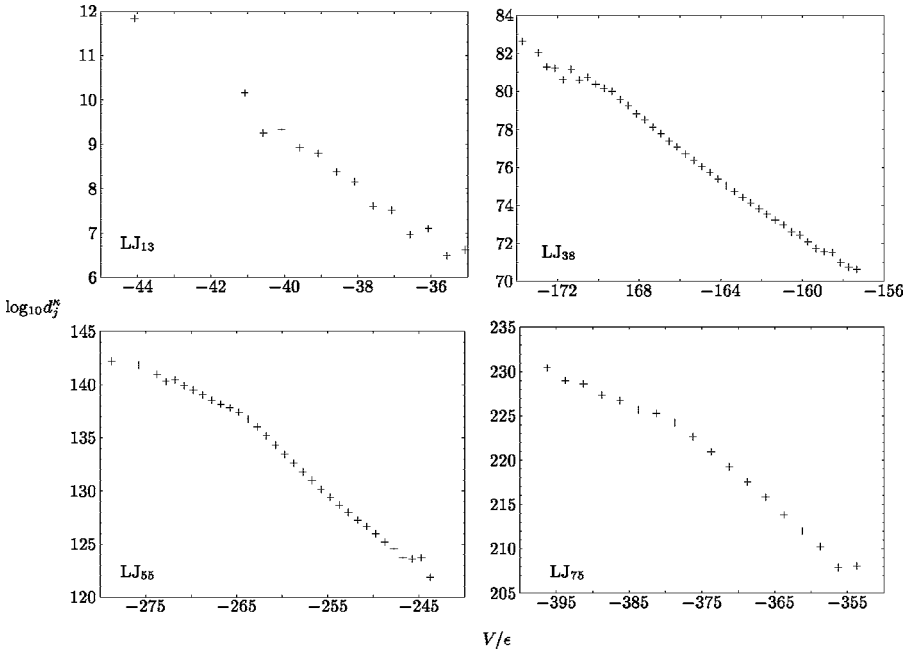

FIG. 9. Dependence of the approximate relative volume of an average basin of attraction $d^{\kappa+3}$ on the potential energy V for four LJ clusters.

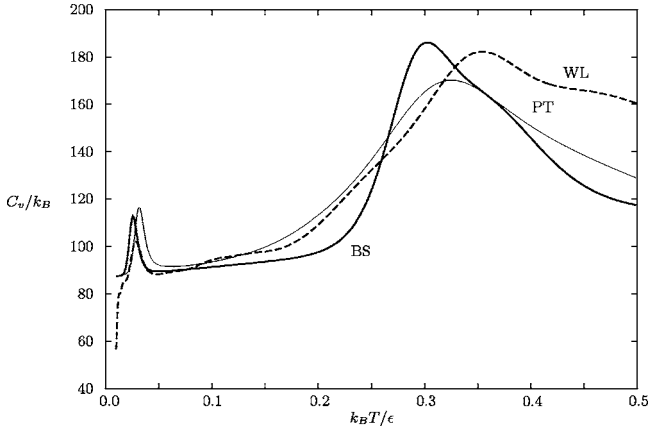

FIG. 10. Heat capacity curves as functions of temperature (in reduced units) for LJ_{31}. The labels are the same as in Fig. 2.

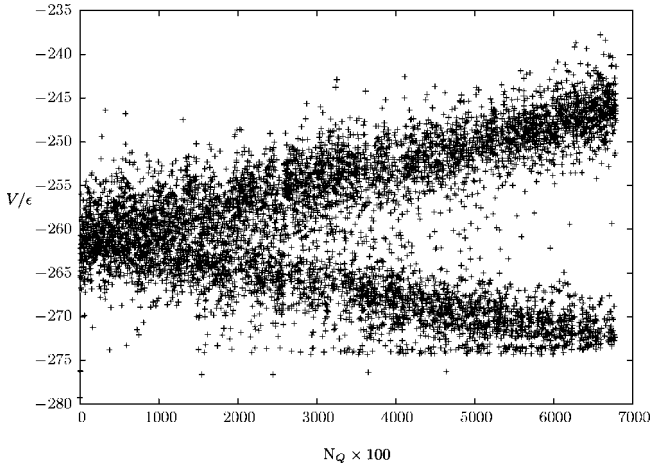

FIG. 11. Scatterplot of the potential energies of local minima sampled for LJ_{55} as a function of time during a BS run. This figure clearly illustrates how the WL procedure initially samples the minima in the density maximum before it samples the tails of the distribution.

B. LJ_{31}

LJ_{31} was chosen because it is the smallest LJ cluster to exhibit broken ergodicity due to a solid-solid phase transition.[1] Such behavior is due to the structure of the global minimum, which is based on icosahedral packing with a Mackay-type overlayer.[1] The competing high-entropy phase is based on local minima with anti-Mackay overlayers.[112] The low temperature peak in the heat capacity calculated using BS agrees well with PT results (Fig. 10). The position of the melting peak is also in reasonable agreement, but the peak height and shape are somewhat different. Since this system is expected to exhibit weak ergodicity breaking it is interesting to compare the timings for BS and PT runs. Table II shows that BS performs well in this case and also for other larger LJ clusters in this table that exhibit double-funnel potential energy surfaces.

C. LJ_{38}

LJ_{38} is probably the best studied double-funnel system. The global potential energy minimum is a face-centered-cubic truncated octahedron, and the next-lowest structure lies in a separate funnel, which is far more densely populated by minima based on icosahedral packing.[1,52,132] Such systems pose significant problems for methods designed to sample the configuration space because of the large potential energy barrier between structures that contribute significantly to the thermodynamics.

Due to the double-funnel character of the PES, and the competition between the low potential energy truncated octahedron and the high-entropy icosahedral region of configuration space, LJ_{38} exhibits a solid-solid transition at low temperature.[52,54,55] This effect is enhanced by the lower vibrational frequencies of the minima based on icosahedral packing, which also increases their entropy. The two funnels are therefore separated by a large free energy barrier at temperatures of interest.[51,53]

Previous thermodynamic studies of LJ_{38} include superposition,[89] J-walking,[111] and PT calculations.[54,55,133,134] Figure 5 compares the heat capacity curves for LJ_{38} obtained by those methods with the current BS results, while Table II shows the convergence times. As expected, reaching convergence in this case requires a significant computational effort, although approximately 12 times less CPU time than PT.

D. LJ_{55}

The global minimum for LJ_{55} is another complete Mackay icosahedron,[129] as for LJ_{13}. The low energy region of the PES again exhibits a palm tree structure,[1] and relaxation to the global minimum is rapid over a wide range of energy or temperature. However, in comparison to LJ_{13}, there is a much larger volume of configuration space to sample.

The melting transition in LJ_{55} has been studied before using Monte Carlo[135,136] and superposition methods,[90] including anharmonic approximations. In the present work we find that T_m predicted by BS is in good agreement with an accurate value calculated using PT (Fig. 5 and Table I). The particularly large heat capacity feature is attributed to the existence of an especially stable global potential energy minimum and is reproduced rather well by BS.

It can be seen from Fig. 11 that the WL walk is confined to the areas of highest potential energy density at the beginning of the simulation. Only when histogram entries in those regions become saturated, do we start to explore the tails of the energy distribution. The density of states for LJ_{55} is rather sharply peaked (Fig. 12); therefore, the energy range that would make a significant contribution to the thermodynamic properties can be established only after several converged WL iterations.

E. LJ_{75}

The PES of LJ_{75} can also be described as a double funnel, featuring a Marks decahedron[137] as the global potential minimum. As for LJ_{38} there is an entropically favored funnel populated by local minima based upon icosahedral packing, and competition between potential energy and entropy again produces a solid-solid transition at low temperature.[112] The available results for comparison in this case are a harmonic superposition calculation of the solid-solid transition

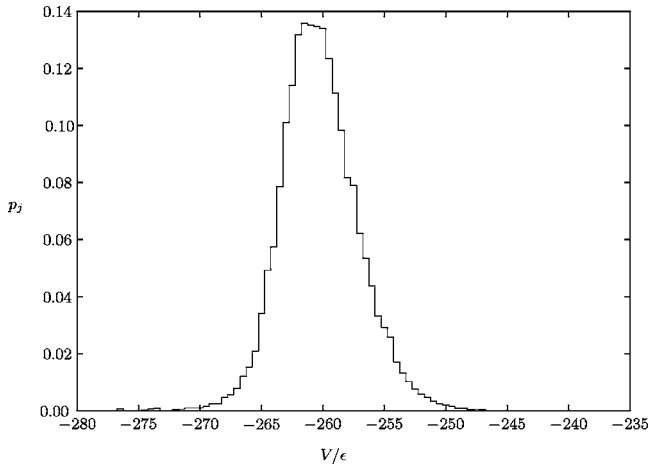

FIG. 12. Normalized probability distribution for the potential energy density of local minima in LJ_{55} as a function of potential energy. The Gaussian-type shape of the distribution is believed to be due to the central limit theorem (Ref. 61).

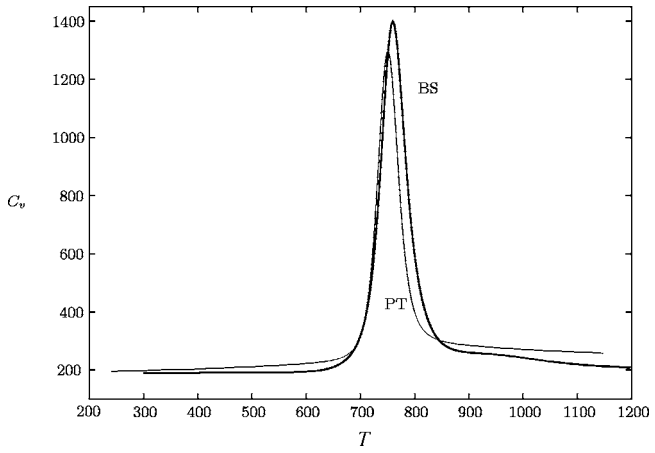

FIG. 13. Heat capacity curve as a function of temperature (in K) for $Na_{32}Cl_{32}$ using BS and PT.

temperature,[6] although some PT results have been reported very recently.[124] This temperature should be quite accurate, since the harmonic approximation should work best at low temperature, and the BS result is within 10% of the previous estimate (Fig. 5 and Table I). To facilitate the transitions between effectively disconnected regions of configuration space corresponding to the global minimum and the icosahedral basin, the density of states was sampled in six overlapping windows. Also, in the calculation of d_j fluctuations due to the large number of configurations at the higher end of potential energy spectrum were removed using a tapered "moving average" data smoothing algorithm.[138]

F. Alkali halide clusters

To test the performance of BS for systems bound by different interatomic forces we have also considered the ionic clusters $(NaCl)_4$, $(NaCl)_{13}Na^+$, and $(NaCl)_{32}$. The Coulomb potential is much longer ranged than the LJ form, and the global minima are based upon cuboidal rocksalt morphologies.[139,140] In fact, the long range of the potential dramatically reduces the number of local minima on the PES, for reasons that are well understood,[1,141,142] making these relatively easy targets for BS. Thermodynamic properties have previously been reported from superposition calculations and molecular dynamics simulations.[143] Additional PT results were obtained for comparison in the present work and were found to agree quite well with the BS results (Fig. 13 and Table I).

V. CONCLUSIONS

The present contribution introduces basin-sampling, a method for calculating classical equilibrium thermodynamic properties. It is based on a Wang-Landau-type accumulation of the potential energy density of local minima using a distance criterion to approximate the volumes of the corresponding basins of attraction, as well as for calculation of anharmonic vibrational partition functions associated with each minimum. Heat capacity curves for selected Lennard-Jones and ionic clusters calculated using the basin-sampling approach are in quantitative agreement with parallel tempering results. Comparison of heat capacity convergence times with those obtained for parallel tempering and conventional Wang-Landau simulations suggests that basin-sampling is particularly advantageous for systems with broken ergodicity. Basin-sampling also provides an insightful connection between the thermodynamics and the underlying features of the potential energy surface. Basin-sampling is implemented in our GMIN.2.1 code, which will be made available in the public domain.[144]

ACKNOWLEDGMENTS

We wish to thank Semen Trygubenko, Jonathan Doye, and Mark Miller for fruitful discussions. One of the authors (T.V.B) is a Cambridge Overseas Trust Scholar.

[1] D. J. Wales, *Energy Landscapes* (Cambridge University Press, Cambridge, 2003).
[2] P. G. Mezey, Theor. Chim. Acta **58**, 309 (1981).
[3] D. J. Wales, J. Chem. Soc., Faraday Trans. **88**, 653 (1992).
[4] D. J. Wales, J. Chem. Soc., Faraday Trans. **89**, 1305 (1993).
[5] Z. Li and H. A. Scheraga, Proc. Natl. Acad. Sci. U.S.A. **84**, 6611 (1987).
[6] D. J. Wales and J. P. K. Doye, J. Phys. Chem. A **101**, 5111 (1997).
[7] D. J. Wales and H. A. Scheraga, Science **285**, 1368 (1999).
[8] D. J. Wales, J. P. K. Doye, M. A. Miller, P. N. Mortenson, and T. R. Walsh, Adv. Chem. Phys. **115**, 1 (2000).
[9] D. J. McGinty, J. Chem. Phys. **55**, 580 (1971).
[10] J. J. Burton, J. Chem. Phys. **56**, 3133 (1972).
[11] M. R. Hoare, Adv. Chem. Phys. **40**, 49 (1979).
[12] F. H. Stillinger and T. A. Weber, Phys. Rev. A **25**, 978 (1982).
[13] F. H. Stillinger and T. A. Weber, Science **225**, 983 (1984).
[14] F. H. Stillinger, J. Chem. Phys. **88**, 7818 (1988).
[15] G. Franke, E. R. Hilf, and P. Borrmann, J. Chem. Phys. **98**, 3496 (1993).
[16] D. J. Wales, Mol. Phys. **78**, 151 (1993).
[17] S. Sastry, P. G. Debenedetti, and F. H. Stillinger, Phys. Rev. E **56**, 5533 (1997).
[18] A. Heuer, Phys. Rev. Lett. **78**, 4051 (1997).
[19] M. Schulz, Phys. Rev. B **57**, 11319 (1998).
[20] S. Sastry, P. G. Debenedetti, and F. H. Stillinger, Nature (London) **393**, 554 (1998).
[21] S. Büchner and A. Heuer, Phys. Rev. E **60**, 6507 (1999).
[22] K. Schröter and E. Donth, Phys. Rev. B **60**, 3686 (1999).
[23] F. Sciortino, W. Kob, and P. Tartaglia, Phys. Rev. Lett. **83**, 3214 (1999).
[24] P. G. Debenedetti, F. H. Stillinger, T. M. Truskett, and C. J. Roberts, J. Phys. Chem. B **103**, 7390 (1999).
[25] C. J. Roberts, P. G. Debenedetti, and F. H. Stillinger, J. Phys. Chem. B

103, 10258 (1999).
[26] S. Büchner and A. Heuer, Phys. Rev. Lett. **84**, 2168 (2000).
[27] W. Kob, F. Sciortino, and P. Tartaglia, Europhys. Lett. **49**, 590 (2000).
[28] F. H. Stillinger, Phys. Rev. E **63**, 011110 (2000).
[29] K. Broderix, K. K. Bhattacharya, A. Cavagna, A. Zippelius, and I. Giardina, Phys. Rev. Lett. **85**, 5360 (2000).
[30] F. Sciortino, W. Kob, and P. Tartaglia, J. Phys.: Condens. Matter **12**, 6525 (2000).
[31] S. Sastry, Phys. Rev. Lett. **85**, 590 (2000).
[32] S. Sastry, J. Phys.: Condens. Matter **12**, 6515 (2000).
[33] B. Coluzzi, G. Parisi, and P. Verrocchio, Phys. Rev. Lett. **84**, 306 (2000).
[34] L.-M. Martinez and C. A. Angell, Nature (London) **410**, 663 (2001).
[35] S. Sastry, Nature (London) **409**, 164 (2001).
[36] F. Sciortino and P. Tartaglia, Phys. Rev. Lett. **86**, 107 (2001).
[37] F. Sciortino and P. Tartaglia, J. Phys.: Condens. Matter **13**, 9127 (2001).
[38] L. Angelani, R. Di Leonardo, G. Parisi, and G. Ruocco, Phys. Rev. Lett. **87**, 055502 (2001).
[39] F. W. Starr, S. Sastry, E. L. Nave, A. Scala, H. E. Stanley, and F. Sciortino, Phys. Rev. E **63**, 041201 (2001).
[40] T. F. Middleton and D. J. Wales, Phys. Rev. B **64**, 024205 (2001).
[41] E. L. Nave, S. Mossa, and F. Sciortino, Phys. Rev. Lett. **88**, 225701 (2002).
[42] S. Mossa, E. La Nave, P. Tartaglia, and F. Sciortino, J. Phys.: Condens. Matter **15**, S351 (2002).
[43] T. Keyes and J. Chowdhary, Phys. Rev. E **65**, 041106 (2002).
[44] F. Sciortino, P. Tartaglia, and W. Kob, Physica A **306**, 343 (2002).
[45] T. F. Middleton and D. J. Wales, J. Chem. Phys. **118**, 4583 (2003).
[46] E. La Nave, F. Sciortino, P. Tartaglia, C. De Michele, and S. Mossa, J. Phys.: Condens. Matter **15**, S1085 (2003).
[47] B. Doliwa and A. Heuer, J. Phys.: Condens. Matter **15**, S849 (2003).
[48] F. Calvo, J. P. K. Doye, and D. J. Wales, J. Chem. Phys. **115**, 9627 (2001).
[49] F. Calvo, J. P. K. Doye, and D. J. Wales, J. Chem. Phys. **114**, 7312 (2001).
[50] J. P. K. Doye and D. J. Wales, Phys. Rev. Lett. **80**, 1357 (1998).
[51] J. P. K. Doye, D. J. Wales, and M. A. Miller, J. Chem. Phys. **109**, 8143 (1998).
[52] J. P. K. Doye, M. A. Miller, and D. J. Wales, J. Chem. Phys. **110**, 6896 (1999).
[53] J. P. K. Doye and F. Calvo, J. Chem. Phys. **116**, 8307 (2002).
[54] J. P. Neirotti, F. Calvo, D. L. Freeman, and J. D. Doll, J. Chem. Phys. **112**, 10340 (2000).
[55] F. Calvo, J. P. Neirotti, D. L. Freeman, and J. D. Doll, J. Chem. Phys. **112**, 10350 (2000).
[56] R. H. Swendsen and J.-S. Wang, Phys. Rev. Lett. **57**, 2607 (1986).
[57] G. Geyer, in *Computing Science and Statistics, Proceedings of the 23rd Symposium on the Interface*, edited by E. K. Keramidas (Inferface Foundation, Fairfax Station, NY, 1991), p. 156.
[58] K. Hukushima and K. Nemoto, J. Phys. Soc. Jpn. **65**, 1604 (1996).
[59] M. C. Tesi, E. J. J. van Rensburg, E. Orlandini, and S. G. Whittington, J. Stat. Phys. **82**, 155 (1996).
[60] U. H. E. Hansmann, Chem. Phys. Lett. **281**, 140 (1997).
[61] J. P. K. Doye and D. J. Wales, J. Chem. Phys. **116**, 3777 (2002).
[62] D. J. Wales and J. P. K. Doye, J. Chem. Phys. **119**, 12409 (2003).
[63] J. P. K. Doye and D. J. Wales, J. Chem. Phys. **102**, 9673 (1995).
[64] K. D. Ball and R. S. Berry, J. Chem. Phys. **111**, 2060 (1999).
[65] F. Wang and D. P. Landau, Phys. Rev. Lett. **86**, 2050 (2001).
[66] F. Wang and D. P. Landau, Phys. Rev. E **64**, 056101 (2001).
[67] D. P. Landau, S.-H. Tsai, and M. Exler, Am. J. Phys. **72**, 1294 (2004).
[68] N. Metropolis, A. W. Rosenbluth, M. N. Rosenbluth, A. H. Teller, and E. Teller, J. Chem. Phys. **21**, 1087 (1953).
[69] D. D. Frantz, D. L. Freeman, and J. D. Doll, J. Chem. Phys. **93**, 2769 (1990).
[70] R. Zhou and B. J. Berne, J. Chem. Phys. **107**, 9185 (1997).
[71] P. Virnau and M. Müller, J. Chem. Phys. **120**, 10925 (2004).
[72] A. P. Lyubartsev, A. A. Martinovski, S. V. Shevkunov, and P. N. Vorontsov-Velyaminov, J. Chem. Phys. **96**, 1776 (1992).
[73] E. Marinari and G. Parisi, Europhys. Lett. **19**, 451 (1992).
[74] B. A. Berg and T. Neuhaus, Phys. Lett. B **267**, 249 (1991).
[75] B. A. Berg and T. Neuhaus, Phys. Rev. Lett. **68**, 9 (1992).
[76] B. A. Berg and T. Çelik, Phys. Rev. Lett. **69**, 2292 (1992).
[77] J. Lee, Phys. Rev. Lett. **71**, 211 (1993).
[78] M.-H. Hao and H. A. Scheraga, J. Phys. Chem. **99**, 2238 (1995).
[79] B. A. Berg, U. H. E. Hansmann, and Y. Okamoto, J. Phys. Chem. **99**, 2236 (1995).
[80] Y. Okamoto and U. H. E. Hansmann, J. Phys. Chem. **99**, 11276 (1995).
[81] H. A. Scheraga and M. H. Hao, Adv. Chem. Phys. **105**, 243 (1999).
[82] U. H. E. Hansmann and Y. Okamoto, Curr. Opin. Struct. Biol. **9**, 177 (1999).
[83] N. Rathore and J. J. de Pablo, J. Chem. Phys. **116**, 7225 (2001).
[84] W. Watanabe and W. P. Reinhardt, Phys. Rev. Lett. **65**, 3301 (1990).
[85] W. P. Reinhardt and J. E. Hunter, J. Chem. Phys. **97**, 1599 (1992).
[86] C. Jarzynski, Phys. Rev. Lett. **78**, 2690 (1997).
[87] M. de Koning, A. Antonelli, and S. Yip, Phys. Rev. Lett. **83**, 3973 (1999).
[88] I. Andricioaei, J. E. Straub, and A. F. Voter, J. Chem. Phys. **114**, 6994 (2001).
[89] J. P. K. Doye, D. J. Wales, and M. A. Miller, J. Chem. Phys. **109**, 8143 (1998).
[90] J. P. K. Doye and D. J. Wales, J. Chem. Phys. **102**, 9659 (1995).
[91] F. Starr, S. Sastry, E. L. Nave, A. Scala, H. Stanley, and F. Sciortino, Phys. Rev. E **63**, 041201 (2001).
[92] S. F. Chekmarev and S. V. Krivov, Chem. Phys. Lett. **287**, 719 (1998).
[93] S. V. Krivov, S. F. Chekmarev, and M. Karplus, Phys. Rev. Lett. **88**, 038101 (2002).
[94] M. S. Shell, P. G. Debenedetti, and A. Z. Panagiotopoulos, Phys. Rev. E **66**, 056703 (2002).
[95] M. S. Shell, P. Debenedetti, and A. Panagiotopoulos, J. Chem. Phys. **119**, 9406 (2003).
[96] T. S. Jain and J. J. de Pablo, J. Chem. Phys. **116**, 7238 (2002).
[97] B. Schulz, K. Binder, M. Müller, and D. P. Landau, Phys. Rev. E **67**, 067102 (2003).
[98] Q. Yan and J. J. de Pablo, Phys. Rev. Lett. **90**, 035701 (2003).
[99] P. Dayal, S. Trebst, S. Wessel, D. Würtz, M. Troyer, S. Sabhapandit, and S. Coppersmith, Phys. Rev. Lett. **92**, 097201 (2004).
[100] F. Calvo, Mol. Phys. **100**, 3421 (2002).
[101] N. Rathore and J. J. de Pablo, J. Chem. Phys. **116**, 7225 (2002).
[102] R. Faller and J. J. de Pablo, J. Chem. Phys. **119**, 4405 (2003).
[103] Q. Yan, T. Jain, and J. J. de Pablo, Phys. Rev. Lett. **92**, 235701 (2004).
[104] E. Mastny and J. J. de Pablo, J. Chem. Phys. **122**, 124109 (2005).
[105] C. Zhou and R. Bhatt, Phys. Rev. E **72**, 025701 (2005).
[106] R. P. White and H. R. Mayne, Chem. Phys. Lett. **289**, 463 (1998).
[107] M. M. Miller, L. M. Amon, and W. P. Reinhardt, Chem. Phys. Lett. **331**, 278 (2000).
[108] J. Nocedal, Math. Comput. **35**, 773 (1980).
[109] D. C. Liu and J. Nocedal, Math. Program. **45**, 503 (1989).
[110] C. J. Tsai and K. D. Jordan, J. Chem. Phys. **99**, 6957 (1993).
[111] D. D. Frantz, J. Chem. Phys. **115**, 6136 (2001).
[112] J. P. K. Doye, M. A. Miller, and D. J. Wales, J. Chem. Phys. **111**, 8417 (1999).
[113] M. de Berg, M. van Kreveld, M. Overmars, and O. Schwarzkopf, *Computational Geometry* (Springer, Berlin, 2000).
[114] D. Avis, D. Bremner, and R. Seidel, Comput. Geom: Theor. Appl. **7**, 265 (1997).
[115] Y. M. Rhee, J. Chem. Phys. **113**, 6021 (2000).
[116] W.-X. Li, T. Keyes, and F. Sciortino, J. Chem. Phys. **108**, 252 (1998).
[117] F. Sciortino and P. Tartaglia, Phys. Rev. Lett. **78**, 2385 (1997).
[118] E. La Nave, A. Scala, F. W. Starr, F. Sciortino, and H. E. Stanley, Phys. Rev. Lett. **84**, 4605 (2000).
[119] S. F. Chekmarev and S. V. Krivov, Phys. Rev. E **57**, 2445 (1998).
[120] H. Lee, Y. Okabe, and D. Landau, e-print cond-mat/0506555.
[121] G. A. Breaux, R. C. Benirschke, and M. F. Jarrold, J. Chem. Phys. **121**, 6502 (2004).
[122] H. Haberland, T. Hippler, J. Donges, O. Kostko, M. Schmidt, and B. von Issendorff, Phys. Rev. Lett. **94**, 035701 (2005).
[123] D. D. Frantz, J. Chem. Phys. **102**, 3747 (1995).
[124] P. A. Frantsuzov and V. A. Mandelshtam, Phys. Rev. E **72**, 037102 (2005).
[125] J. P. Neirotti, D. L. Freeman, and J. D. Doll, J. Chem. Phys. **112**, 3990 (2000).
[126] M. A. Miller, J. P. K. Doye, and D. J. Wales, J. Chem. Phys. **110**, 328 (1999).
[127] J. E. Jones and A. E. Ingham, Proc. R. Soc. London, Ser. A **107**, 636 (1925).
[128] M. P. Tosi and F. G. Fumi, J. Phys. Chem. Solids **25**, 45 (1964).
[129] A. L. Mackay, Acta Crystallogr. **15**, 916 (1962).
[130] M. A. Miller and D. J. Wales, J. Chem. Phys. **107**, 8568 (1997).
[131] J. P. K. Doye and C. P. Massen, J. Phys. Chem. **122**, 084105 (2005).

[132] D. J. Wales, M. A. Miller, and T. R. Walsh, Nature (London) **394**, 758 (1998).
[133] C. Predescu, P. A. Frantsuzov, and V. A. Mandelshtam, J. Chem. Phys. **122**, 154305 (2005).
[134] H. B. Liu and K. D. Jordan, J. Phys. Chem. B **109**, 5203 (2005).
[135] P. Labastie and R. L. Whetten, Phys. Rev. Lett. **65**, 1567 (1990).
[136] V. V. Nauchitel and A. J. Pertsin, Mol. Phys. **40**, 1341 (1980).
[137] L. D. Marks, Philos. Mag. A **49**, 81 (1984).
[138] J. F. Kenney and E. S. Keeping, *Mathematics of Statistics*, 3rd ed. (Van Nostrand, Princeton, NJ, 1962), pt. 1.
[139] J. G. Nourse, J. Am. Chem. Soc. **102**, 4883 (1980).
[140] A. Ayuela, P. W. Fowler, D. Mitchell, R. Schmidt, G. Seifert, and F. Zerbetto, J. Phys. Chem. **100**, 15634 (1996).
[141] P. A. Braier, R. S. Berry, and D. J. Wales, J. Chem. Phys. **93**, 8745 (1990).
[142] J. P. K. Doye and D. J. Wales, J. Chem. Soc., Faraday Trans. **93**, 4233 (1997).
[143] J. Anwar, D. Frenkel, and M. Noro, J. Chem. Phys. **118**, 728 (2003).
[144] D. J. Wales, *GMIN*, A program for finding global minima; http://www-wales.ch.cam.ac.uk/GMIN